

Hyperon Radii

B. POVH

*Max-Planck-Institut für Kernphysik,
Post Box 103980
D-69029 HEIDELBERG
E-mail: b.povh@mpi-hd.mpg.de*

A survey of the experimental data on the charge and strong hadronic radii is given. A new, however preliminary value of the Σ^- charge radius allows to include also hyperons in the systematics. The presented data on the hadronic radii give the first hint of their dependence on the strangeness content. An estimate of the constituent quark size is given.

1 Introduction

Constituent quark models, nonrelativistic and semi-relativistic, reproduce well the static properties and low excitations of hadrons. Probably the most convincing support of the constituent quark concept is the impressive agreement between the model predictions for the magnetic moments and the data. The data on the baryon octet, six measured magnetic moments in total, give a sufficient constraint to the predictions of the model to make the concept of the constituent quark credible. It has essentially two free parameters, the light and the strange quark mass. Here we do not count the parameters of the quark-quark potential which is assumed to be such that the kinetic and the potential energy cancel each other.

Hadronic radii can supply us with further information on the constituent quark properties. The sizes of the hadrons are given by the sizes of the constituent quarks and the confinement forces. Again, if the charge radii of the hyperons were determined, we would get five independent data points on the dependence of the hyperon radii on the content of the strangeness: four by replacing the light quarks in the nucleon by the strange ones, the fifth by comparing the Σ^+ and Σ^- which should have different charge radii because the u- and d-quarks in the two hyperons lead to a different charge distribution.

The aim of this paper is twofold. Firstly, by presenting the determination of the charge radius of Σ^- we show that a systematic measurements of hyperon radii is feasible with present experimental techniques and existing hyperon beams. Secondly, by comparing charge and strong radii, the latter obtained from the hadronic cross sections, we demonstrate the equivalence between the two.

The presented data on the hadronic radii give the first hint of their dependence on the strangeness content and on the quark sizes.

2 Σ^- -Electron Scattering

The first measurement of charge radii of unstable particles, pion and kaon, was performed at CERN in the early 80's by Amendolia *et al.*^{1,2}. Negative pions and kaons of 300 GeV were scattered on electrons of a liquid hydrogen target. The angles of the scattered mesons and recoil electrons were measured by a set of wire chambers, the momenta by the following magnetic spectrometer.

Intense hyperon beams operate at the highest possible energies in order to increase the decay length of the hyperons. A high hyperon energy is also vital for the measurement of the electromagnetic form factors in order to obtain scattering events with a sufficiently high Q^2 bite to deduce at least the charge radius, the first moment of the charge distribution. The beam used by the SELEX collaboration at Fermilab was tuned to 600 GeV. At this momentum of Σ^- the energy of the recoil electrons range from 0 to 180 GeV, while the largest angle for the scattered Σ^- is 0.5 mrad and for the recoiling electrons 8 mrad in the momentum acceptance of the spectrometer. A typical scattering event is shown in Fig. 1.

In Fig. 1, only the part of the SELEX experiment relevant for the identification of the scattering events is shown. The momenta and angles of the incoming Σ^- were determined by reconstructing the beam tracks in the set of silicon strip detectors in front of the target, the scattering angles by the detector behind the target. The momenta of the scattered particles were obtained by the reconstruction of the particle trajectories in the following two magnetic spectrometers. Silicon strip detectors, 5 cm in diameter, were positioned behind the first and in front of and behind the second magnet.

An average uncertainty in the determination of the scattering angle was 30 μ rad, and the momentum for the Σ^- was determined by an accuracy of $\approx 1\%$. The four-momentum transfer Q^2 was calculated by using the scattering angles of the Σ^- , of the recoiling electron and the Σ^- momentum. The electron momentum was not fully used in the analysis because of large radiation corrections to be applied to it.

The experimentally obtained cross sections have been fitted to the following formula:

$$\left(\frac{d\sigma}{dQ^2}\right)_{exp} = \left(\frac{4\pi\alpha}{Q^4} \left(1 - \frac{Q^2}{Q_{max}^2}\right)\right)_{Mott} \cdot F^2(Q^2). \quad (1)$$

The form factor $F(Q^2)$ depends on the electric and the magnetic form factor.

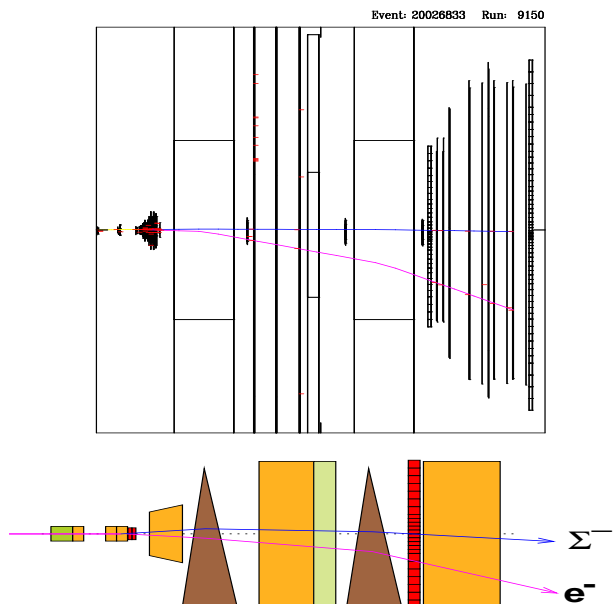


Figure 1: Event display of an elastic Σ^- -e scattering event in the SELEX detector.

As generally used in the electron-proton scattering and also for the Σ^- the Sachs form factors with the empirical dipole dependence on Q^2 are assumed:

$$G_E(Q^2) = \frac{1}{\kappa - 1} G_M(Q^2) = \left(1 + \frac{1}{6} Q^2 \langle r_{ch}^2 \rangle\right)^{-2}. \quad (2)$$

In the case of Σ^- the anomalous magnetic moment $\kappa = -0.16$ is very small. In Fig. 2, the Q^2 dependence of the cross section is shown for different radii.

Because of the large variation in data for the proton charge radius (see Tab. 1) from various experiments, indicating uncontrolled systematic errors, it was felt that the Σ^- charge radius should be compared to the proton radius obtained in the same experiment. The preliminary value for the Σ^- radius is $\langle r_{ch}^2 \rangle_{\Sigma^-} = (0.60 + 0.08(stat.) + 0.08(syst.)) \text{ fm}^2$ and for the proton $\langle r_{ch}^2 \rangle_p = (0.84 + 0.09(stat.) + 0.06(syst.)) \text{ fm}^2$. In spite of the large errors the results strongly indicate that the Σ^- radius is smaller than that of the proton.

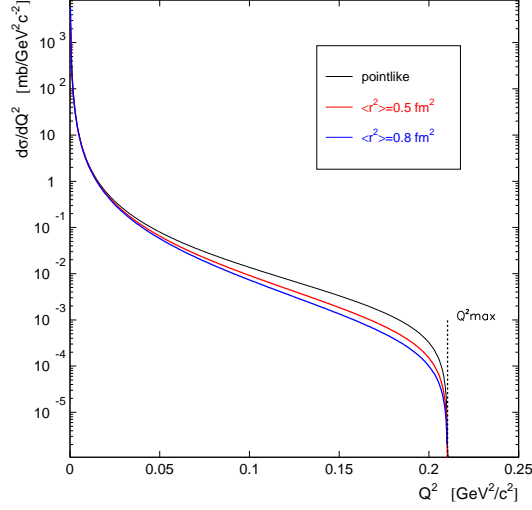


Figure 2: Differential cross section of elastic Σ^- -e scattering at 650 GeV/c.

3 Charge vs. Strong Radii

A meson interacts with a nucleon like a colour dipole. A baryon can also be viewed as a coherent sum of colour dipoles. Therefore, it is expected that the total cross sections of hadrons on a nucleon are proportional to the $\langle r^2 \rangle_h$ of the hadron. It was shown by Povh and Hüfner³ that at sufficiently high energies, $\sqrt{s} \geq 20\text{GeV}$, the total cross section of hadrons on the nucleon are given by

$$\frac{\sigma(h, p)}{\sigma(p, p)} \simeq \frac{\langle r^2 \rangle_h}{\langle r^2 \rangle_p}, \quad (3)$$

providing the cross sections are measured at the same energies. The total hadronic cross sections grow logarithmically with energy. This is the consequence of the gluon halo of which softer and softer components interact with increasing energy (Hüfner and Povh⁴). It is not possible to define an energy independent strong radius, but a good fit to the data is obtained assuming

$$\langle r^2(s) \rangle_{strong} = \langle r^2 \rangle_{ch} \cdot \left(\frac{s}{s_0} \right)^\Delta. \quad (4)$$

Δ has a value of about 0.1. The correspondence between the strong and charge radii is shown in Fig. 3. The total cross sections and the strong radii deduced

from them are better and more abundantly measured than the charge radii. Therefore, in the following discussion we will combine the information from the two sources in order to discuss the flavour dependence of the hadronic sizes.

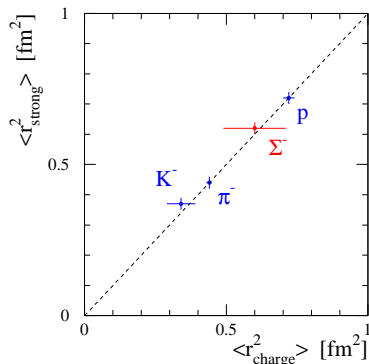


Figure 3: Strong versus measured electromagnetic charge radii of hadron.

4 Flavour Dependence of the Hadronic Radii

The charge radius gives the first moment of the charge distribution, the strong, as defined above, the first moment of the mass distribution. The two are in general not the same because the quarks have different electric charges but the same strong coupling. Nevertheless, for all the hadrons quoted in Tab. 1, the two radii are the same if properly scaled. This scaling is done by adjusting the strong radius of proton to be equal to its charge radius. In the following discussion we will just talk about the hadronic radii. In fact, the only exception in the family of hyperons is Σ^+ which is expected to have the charge radius larger than the strong one. This is because the two *up* quarks with the summed charge of 4/3 units surround the *strange* quark that very likely has smaller extension than the light quarks.

Let us denote the mass distribution of the light quarks with $\Phi(q)$ and for the strange quark with $\Phi(s)$. The radii of the hadrons in the right column of the Table 1. can be written as:

$$\langle r^2 \rangle_p = \int \Phi_h(q) r^2 d^3 r \quad (5)$$

$$\langle r^2 \rangle_{\Sigma^-} = \int [2/3 \Phi_h(q) + 1/3 \Phi_h(s)] r^2 d^3 r \quad (6)$$

Table 1: Comparison of measured electromagnetic charge radii to strong interaction radii

	mean square radius [fm ²]	
	electromagnetic interaction	strong interaction
p	0.74 ± 0.02 ⁵	0.72 ± 0.02
p	0.79 ± 0.03 ⁶	
p	0.72 ± 0.01 ⁷	
n	-0.11 ± 0.03 ⁸	
Σ^-	0.9 ± 0.5 ⁹	0.62 ± 0.02
Ξ^-		0.54 ± 0.02
π^-	0.44 ± 0.01 ¹	0.43 ± 0.02
K^-	0.34 ± 0.05 ²	0.37 ± 0.02
K^0	-0.054 ± 0.026 ¹⁰	

$$\langle r^2 \rangle_{\Xi^-} = \int [1/3\Phi_h(q) + 2/3\Phi_h(s)]r^2 d^3r \quad (7)$$

$$\langle r^2 \rangle_{\pi^-} = \int 2/3\Phi_g(q)r^2 d^3r \quad (8)$$

$$\langle r^2 \rangle_{K^-} = \int 1/3[\Phi_g(q) + \Phi_g(s)]r^2 d^3r. \quad (9)$$

Here we assumed that in the first approximation $\Phi_h(q)$ and $\Phi_h(s)$ do not depend strongly on the number of the strange quarks in the hyperon. On the other hand, $\Phi_g(q)$ and $\Phi_g(s)$, the density distributions of the Goldstone particles π^- and K^- certainly differ from those of the hyperons in the contribution coming from the relative motion of the quarks.

The differences of the square radii:

$$\langle r^2 \rangle_p - \langle r^2 \rangle_{\Sigma^-} \quad (10)$$

$$\langle r^2 \rangle_{\Sigma^-} - \langle r^2 \rangle_{\Xi^-} \quad (11)$$

$$\langle r^2 \rangle_{\pi^-} - \langle r^2 \rangle_{K^-} \quad (12)$$

have, within the experimental errors, the same value, $\Delta\langle r^2 \rangle = 0.1 \pm 0.03$. Thus we can write

$$\int [\Phi_h(q) - \Phi_h(s)]r^2 d^3r \simeq \int [\Phi_g(q) - \Phi_g(s)]r^2 d^3r = 0.3 \pm 0.09 fm^2. \quad (13)$$

This result implies a very strong radius dependence on the quark mass. If the density distribution were only the consequence of the relative motion of the

quarks in the hyperon the mass dependence of the radius were rather weak. The fact that the $\Delta\langle r^2 \rangle$ are approximately equal in the hyperons and the Goldstone bosons suggests that the major part of this difference is due to the different intrinsic radii of the constituent light and strange quarks.

It was pointed out by Povh and Hüfner¹¹ that in the nonrelativistic quark model the hadronic excitations and the hadronic radii are consistently described if one attributes an apparent radius to each constituent quark, $\langle r^2 \rangle_{u,d} = 0.36 \text{ fm}^2$ for the light and $\langle r^2 \rangle_s = 0.16 \text{ fm}^2$ for the strange quark. This result is not surprising. The radius of a nonrelativistic quark is just the Compton wave length of the quark, $\langle r^2 \rangle^{1/2} \approx \frac{1}{m_q}$, which is rather obvious for a confined particle. The virtual creation of quark-antiquark pairs in the confining field leads to a fluctuation ("Zitterbewegung") in the position coordinate of the quark, which appears in the nonrelativistic Schrödinger picture as an apparent size of the moving quark, with a value close to the Compton wave length. This effect has been calculated by Hayne and Isgur¹² for the non-relativistic quark model.

In conclusion we want to point out that the same quark masses used to optimise the magnetic moments and the low lying excited states of the hyperons do give an excellent result for the hadronic radii if one assumes an intrinsic radius of the constituent quark to have the value of its Compton wave length.

Acknowledgments

I would like to thank my colleagues H. Krüger, J. Simon and G. Dirkes for supplying me with the results of the SELEX experiment.

References

1. S.R. Amendolia *et al.*, *Nucl. Phys. B* **277**, 168 (1986).
2. S.R. Amendolia *et al.*, *Phys. Lett. B* **178**, 435 (1986).
3. B. Povh, J. Hüfner, *Phys. Rev. Lett.* **58**, 1612 (1987).
4. J. Hüfner, B. Povh, *Phys. Lett. B* **215**, 772 (1988).
5. G. Simon, C. Schmitt, F. Borkowski, V. Walther, *Nucl. Phys. A* **333**, 381 (1980).
6. T. Udem *et al.*, *Phys. Rev. Lett.* **79**, 2646 (1997).
7. P. Mergell, U.G. Meissner, D. Drechsel, *Nucl. Phys. A* **596**, 367 (1996).
8. L. Köster, *Phys. Rev. Lett.* **36**, 1021 (1976)
9. M.I. Adamovich *et al.*, *Eur. Phys. J. C* **8**, 59 (1999)
10. W.R. Molzon *et al.*, *Phys. Rev. Lett.* **41**, 1213 (1978)
11. B. Povh, J. Hüfner, *Phys. Lett. B* **245**, 653 (1990).
12. C. Hayne, N. Isgur, *Phys. Rev. D* **25**, 1944 (1982).